ORIGINAL PAPER

Synthesis of superabsorbent composite based on chitosan-g-poly(acrylamide)/attapulgite

El-Refaie Kenawy[1] · Hasnaa Hasab Elnaby[1] · Mohamed M. Azaam[1]

© The Author(s) 2023

Abstract

The production of environmentally friendly SAP using biodegradable natural resources such as chitosan was synthesized for water saving and controlled-released fertilizer. Chitosan-g-poly(acrylamide)/attapulgite superabsorbent composites (CTS) were created by crosslinking *N,N'*-methylene-bis-acrylamide (MBA) with chitosan (Ch), acrylamide, and attapulgite (ATP) and initiating the reaction with potassium persulfate (KPS). Spectroscopic techniques such as Fourier transform infrared spectroscopy, thermal gravimetric analysis (TGA), and scanning electron microscope were used to characterize the composite structures. It was done to determine how certain characteristics, such as the initiator percentage, crosslinker ratio, and clay content, affected the composite's ability to swell. The results confirmed that the thermal stability of the composite was improved by the addition of ATP. The maximum swelling was attained when the KPS concentration was 0.1 g. However, the addition of 0.2 g of KPS created a composite with a lower swelling capacity. When the amount of ATP was increased by up to 0.4 g, the swelling increased from 210 to 319 g/g. However, as the clay amount was increased further to 1.2 g, the swelling capacity decreased to 170 g/g. As pH increased to 3.0, the swelling of ATP2 grew larger; nevertheless, it shrank between pH values of 3 and 6. As the pH climbed to 8, the swelling sharply grew. The chosen composition was evaluated as a controlled-release method for urea fertilizer and swelled to 319 g/g in water (CTS2). The findings demonstrated that when the formulation's ATP content was increased from 0 to 1.2 g, the release rate was delayed, and the release length increased from 5 to 21 h.

✉ El-Refaie Kenawy
    ekenawy@yahoo.com

✉ Mohamed M. Azaam
    mmkazaam@yahoo.com

[1] Polymer Research Group, Department of Chemistry, Faculty of Science, Tanta University, Tanta, Egypt

Graphical abstract
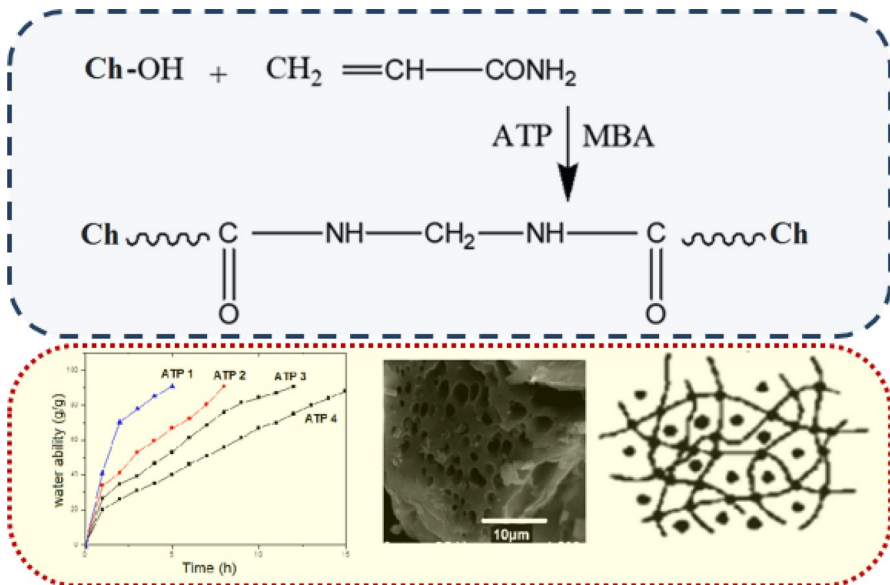
Introduction

Due to the existence of several hydrophilic groups on the polymer chains, such as COOH, NH$_2$, CONH, OH, and SO$_3$H, superabsorbent polymers that can absorb and hold enormous amounts of water have attracted a lot of attention in recent years [1]. The majority of SAPs are built using acrylamide (AM), which offers the advantage of excellent salt resistance in terms of raw material performance. The usage of SAPs is growing, as are their requests in areas such as water treatment, drug delivery systems, and other specialized industries. Examples of these industries include hygienic and bio-related products (most commonly one-use diapers and female napkins), agriculture and horticulture (controlled release of agrochemicals in soil), and disposable diapers and pads [2, 3]. A layered aluminum silicate (with reactive OH groups on the surface) is attapulgite. As a result, it is a useful substrate for materials that are extremely absorbent and is less sensitive to salts than other clays [4, 5]. Technological developments related to SAP are anticipated to enable the production of environmentally friendly SAP using biodegradable natural resources. Ch is a natural, linear polysaccharide with strong biocompatibility, biodegradability, and antibacterial properties [6].

The second greatest prevalent natural polymer in the world after cellulose is Ch, a copolymer of *N*-acetylglucosamine and *N*-glucosamine units dispersed arbitrarily or in blocks across its chains [7]. It possesses a number of intriguing qualities, including the capacity to form gels and films as well as bio-adhesion, biodegradability, and biocompatibility [8–11]. Additionally, Ch antibacterial possessions against a diversity of bactericides and fungi are prejudiced by frequent factors, including water solubility, pH level, and molecular weight [12, 13]. As a result, Ch and other superabsorbent may have antibacterial properties and so be utilized in hygienic products [14]. Especially for drug delivery, chitosan and its derivatives have been employed widely in the production of biomedical products, cell immobilization, and enzymes [15]. Prior to now, many SACs made of chitosan were created to achieve highly absorbent capacities. For instance, a brand-new chitosan-g-poly(acrylic acid)/attapulgite superabsorbent composite was created, having water absorbency of 159.6 g g^{-1} in water and 42.3 gg^{-1} in 0.9 wt% NaCl solution [16].

Due to its high nitrogen concentration (46.4%) and comparatively low price, urea is the fertilizer most commonly used in agriculture to enhance crop growth [17]. By the way, nitrogen leaching and ammonia emission from the application of raw urea to the soil might result in pollution and economic loss [18]. So, it is in everyone's best interest; both economically and environmentally to develop slow- or controlled-release urea systems made of sustainable materials. Silicate minerals, such as bentonite, attapulgite, and montmorillonite, and organic polymers, such as polyacrylamide (PAM), have been proposed for the manufacturing of slow-release urea fertilizers [19–22]. The integration of nutrients in hydrogels allows enhancing crops nutrition while minimizing the environmental impact owing to leaching of water-soluble fertilizers, since also reduce evaporation losses and decrease the frequency of irrigation. The ingredients (Ch), acrylamide (AM), and attapulgite (ATP) clay were used to create SACs in the current study. Investigations were also conducted into the composites' urea release.

Experimental

Materials

Ch, AM, and MBA were acquired from an organics company in New Jersey (USA) and used as received. KPS, urea, and NaOH were obtained from El-Nasr Pharmaceutical Co. (Egypt). ATP was marketed by the Southern Clay Corporation in the US.

Synthesis of superabsorbent composites

A series of samples having varied amounts of ATP, MBA, KPS, and AM were made using the following procedure:

(0.5–1.2 g) Ch was added to 20 mL of distilled water. KPS (0.05–0.2 g) was added to the combined solution and agitated for 15 minutes at 70 °C. A mixture

of (4.0–6.0 g) AM, (0.006 g) MBA, and (0–1.2 g) ATP was used. After 30 minutes, the completed product was added to a NaOH solution (2 mol/L) and reacted for 2 h at 80–90 °C before being hydrolyzed. In order to get rid of any base, monomer, or ungrafted molecules, the product was rinsed using pure water. Following a second round of purification with methanol washing, the recovered product was ground, stored away from moisture, heat, and light after being dried for 10 h at 70°C. This reaction was carried out by altering the amounts of the constituents, as shown in Table 1.

Characterization techniques

With the TENSOR 27-Series, KBr pellet, and Bruker, FT-IR was captured (from 400 to 4000 cm^{-1}).

Cu-K radiation (at λ 0.1541 nm) was used to produce XRD spectra by the GNR APD-2000 (40 kV, 30 mA, and 2θ of 2–15°). Shimadzu's TGA-50 (temperature rate 10 °C/min) was used to perform the TGA. The products were covered with gold at reduced pressure and examined under a SEM using JSM6510 JEOL 30Kv. A Biosystem BTS 350 with a full spectrum of LEDS was used to track the release of urea (340, 405, 505, 535, 560, 600, 635, and 670 nm). The samples were dried in a vacuum oven (BINDER, Germany) before to examination.

Table 1 Composition and swelling capacity of the various composites

Sample	KPS (g)	AM (g)	ATP (g)	Ch (g)	MBA (g)	Water ability (g/g)
CTS1	0.1	6.0	0	0.5	0.006	260
CTS2	0.1	6.0	0	0.8	0.006	319
CTS3	0.1	6.0	0	1.0	0.006	250
CTS4	0.1	6.0	0	1.2	0.006	180
ATP1	0.1	6.0	0	0.8	0.006	210
ATP2	0.1	6.0	0.4	0.8	0.006	319
ATP3	0.1	6.0	0.8	0.8	0.006	240
ATP4	0.1	6.0	1.2	0.8	0.006	170
AM1	0.1	4.0	0.4	0.8	0.006	140
AM2	0.1	4.5	0.4	0.8	0.006	205
AM3	0.1	5.0	0.4	0.8	0.006	270
AM4	0.1	6.0	0.4	0.8	0.006	319
KPS1	0.05	6.0	0.4	0.8	0.006	275
KPS2	0.1	6.0	0.4	0.8	0.006	319
KPS3	0.15	6.0	0.4	0.8	0.006	290
KPS4	0.2	6.0	0.4	0.8	0.006	230

Water absorbency measurement

To achieve the swelling equilibrium, a weight amount of the superabsorbent composite was submerged in distilled H_2O or saline solutions. After that, swollen products were filtered using a 70-mesh screen (30 minutes) to remove any residual H_2O [23]. The superabsorbent composite's H_2O absorption (QH_2O) was projected by means of the formula:

$$QH_2O = (m_2 - m_1)/m_1$$

where $m2$ is the product weight after being swollen by H_2O, and m1 is the dry product weight. The amount of water in one gram of product, or QH_2O, was calculated.

Loading of urea onto the produced superabsorbent composite

This process involved adding 0.1 g of dried gel samples (APT1, APT2, APT3, and APT4) into an aqueous solution of 0.5 M urea. For a full day, this solution was allowed to swell. At 60 °C, the swelled gels were dried.

Study the release of urea from loaded superabsorbent composite in distilled H_2O

At room temperature, 100 mL of distilled H_2O (the release medium) was added to the 0.1 g of loaded gel. Urea concentrations in the solutions were measured using the biosystem method, and at various times, the amount of urea released was calculated.
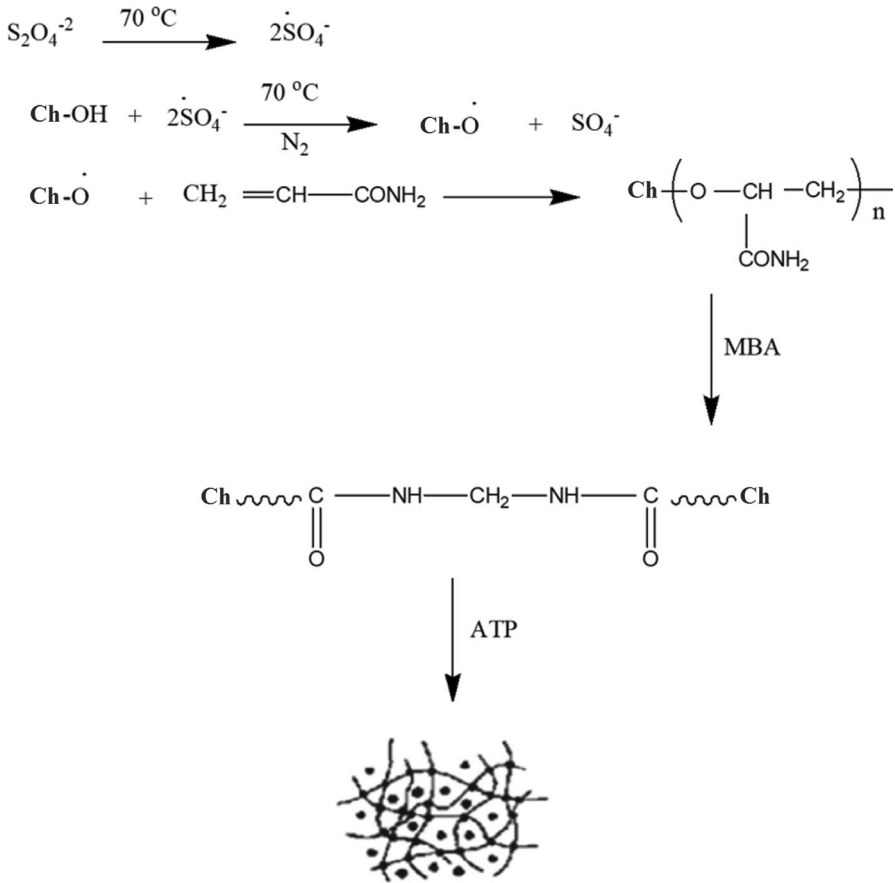
Results and discussion

Scheme 1 shows the mechanism of the graft copolymerization of AM onto Ch. By heating the persulfate, sulfate anion radicals are produced. These radicals create alkoxy radicals, which are able to start the free radical polymerization of AM, by removing hydrogen from the OH groups of the chitosan backbones. To create the final composite, chitosan-grafted crosslinked AM interacted with ATP further.

Characterization of the superabsorbent composite

By using FT-IR, XRD, TGA, and SEM, the composites' structural characteristics were identified.

FT-IR was used to pinpoint the functional groups in unmodified chitosan [24]. Figure 1 displays the FT-IR of CTS2 and CTS3. An absorption band at 2957 cm^{-1} was attributed to CH stretching. Symmetric COO$^-$ stretching is absorbed at 1415 cm^{-1}. Band at 1562 cm^{-1} was caused by asymmetric COO$^-$ stretching, representing

$$S_2O_4^{-2} \xrightarrow{70\ ^\circ C} 2\dot{S}O_4^{-}$$

$$\text{Ch-OH} + 2\dot{S}O_4^{-} \xrightarrow[N_2]{70\ ^\circ C} \text{Ch-}\dot{O} + SO_4^{-}$$

$$\text{Ch-}\dot{O} + CH_2{=}CH{-}CONH_2 \longrightarrow Ch\left(O{-}CH{-}CH_2\right)_n$$
$$\overset{|}{C}ONH_2$$

MBA

$$\text{Ch}\sim\sim\sim\overset{\text{C}}{\underset{\parallel}{}}{-}NH{-}CH_2{-}NH{-}\overset{\text{C}}{\underset{\parallel}{}}\sim\sim\sim\text{Ch}$$
$$\overset{}{O}\qquad\qquad\qquad\overset{}{O}$$

ATP

Scheme 1. The suggested grafting mechanism for AM and Ch

the chemical environment of COO⁻ has changed, which might have some influence on the superabsorbent composite in capability to absorb [25].

The XRD technique was used to characterize the unmodified chitosan [24]. Figure 2 displays the XRD of ATP and Ch-g-PAM/ATP. The basal d-spacing of 1.30 nm and a significant reflection of ATP at $2\theta = 6.76$ are shown [26–28]. This reflection of ATP is still observed in the composite's diffraction pattern after grafting with Ch-g-PAM/ATP without noticeable shift. This outcome suggests that during polymerization, the crystalline structure of ATP was preserved.

Figure 3 displays the TGA of Ch-g-PAM and Ch-g-PAM/ATP composites. Between 100 and 200 °C, the adsorbed water lost weight, saccharide rings dehydrated, and the C-O-C glycosidic linkages in the main chain of CTS broke down [29–32]. The breakdown of the carboxyl groups in PAM chains was the cause of the weight losses in the 280–560 °C range. The addition of ATP to the polymer network caused the final stable to develop around 560–800 °C. The TGA of
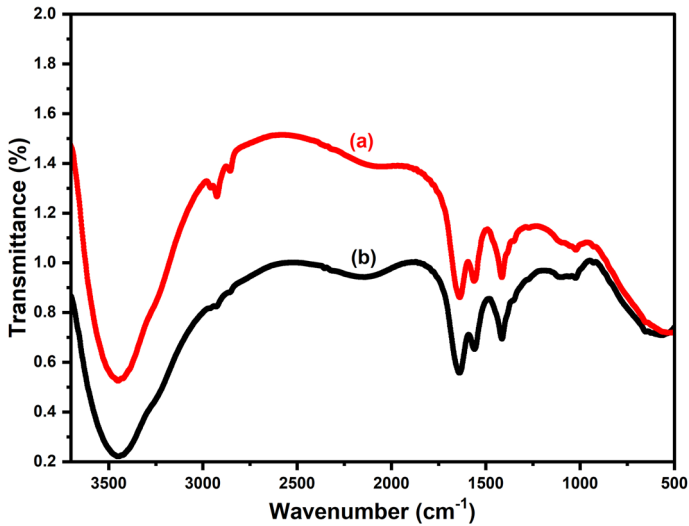
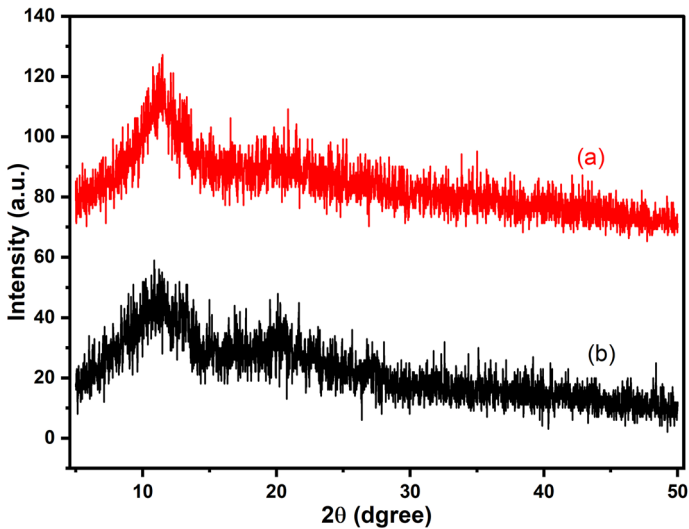**Fig. 1** FT-IR spectra of **a** CTS3 and **b** CTS2

Fig. 2 XRD of **a** ATP and **b** Ch-g-PAM/ATP

the Ch-g-PAM and Ch-g-PAM/ATP revealed that the latter's thermal stability had increased as a result of the addition of ATP. For instance, the residual weight of Ch-g-PAM at 600 °C was around 12%, whereas the remaining from Ch-g-PAM/ATP was about 20%. These findings supported the notion that the addition of ATP increased the composite's thermal stability.
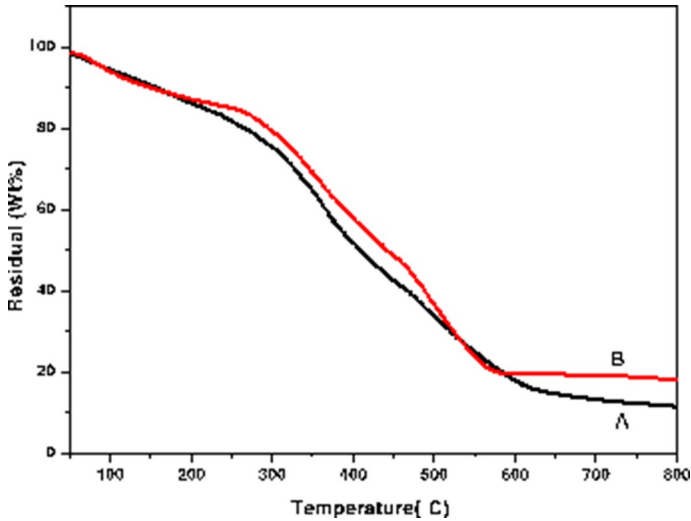
Fig. 3 TGA of Ch-g-PAM and Ch-g-PAM/ATP

SEM was used to examine the morphological properties of unmodified chitosan [24].

Figure 4 displays the Ch-g-PAM/ATP (CTS2) SEM images. It has been detected that the capability of superabsorbent composites to absorb H_2O and swell is prejudiced by the existence of a rough surface occupied with spaces.

Reaction parameter impact on water absorption

On composite swelling ability, the impact of several parameters including KPS, AM, ATP, chitosan quantities, and aqueous medium pH was examined.

The effect of the KPS amount

The prepared SACs' water absorbency was examined in relation to the effect of the initiator, which ranges from 0.05 to 0.2 g (Figure 5 and Table 1).

Due to an increase in free radicals caused by the increase in initiator amount (from 0.05 to 0.1 g), water absorbance rose, which, in turn, increased the likelihood that AM would react with Ch. When the KPS concentration reached 0.1 g, the greatest swelling was attained. However, by increasing the amount of KPS to 0.15 g, the swelling ability was reduced. The addition of 0.2 g of KPS, which produced a composite with a decreased swelling ability, validated this observation. This is because there are additional free radicals present, which hasten the chain termination and diminish water absorption [33].
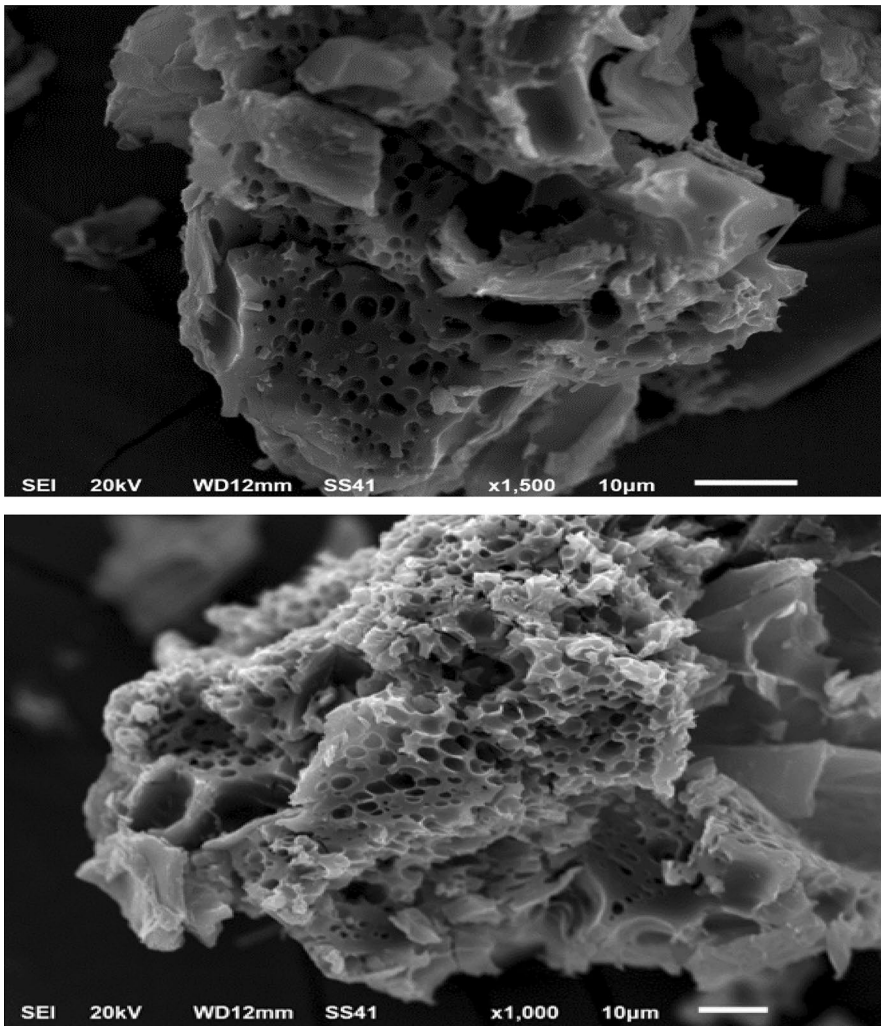
Fig. 4 SEM images at diverse magnitude (X 1000 and X 1500) of CTS2

The effect of AM amount

By adjusting the AM quantity from 4.0 to 6.0 g, the impact of AM amount on the produced composite's swelling ability was examined (Table 1). The outcomes showed that raising the AM monomer concentration (from 140 to 319 g/g) increased the swelling ability (Figure 6). The increasing availability of monomer molecules close to the chain-propagating sites of chitosan macromolecules may be the cause of this rise in swelling.
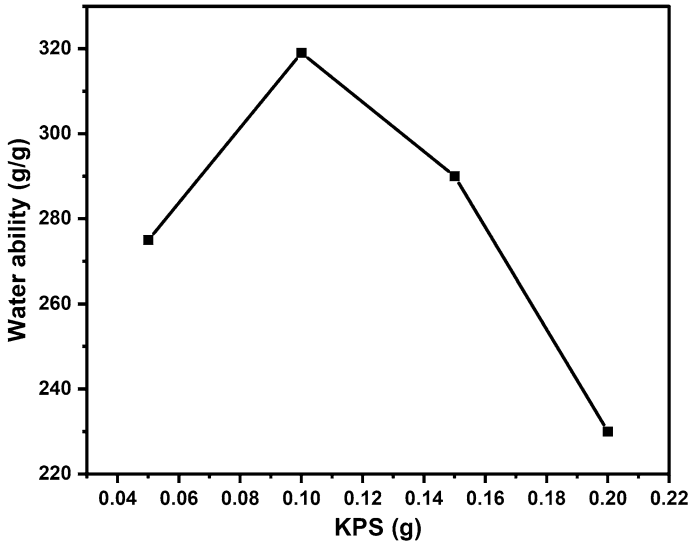
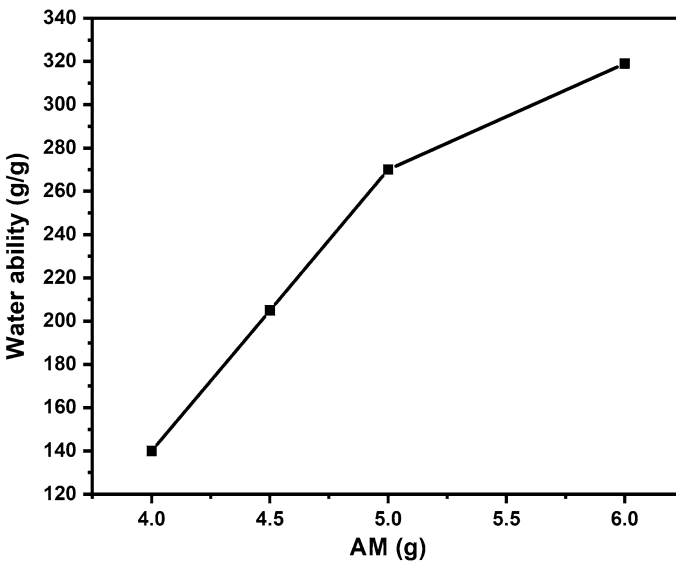**Fig. 5** Effect of KPS content on the composite swelling

Fig. 6 Effect of AM content on the composite swelling capacity

The effect of ATP clay

Different concentrations of ATP (0–1.2 g) were added to the composites to study the impact of clay on their ability to swell. Figure 7 demonstrates that swelling rose as ATP levels rose. This might be because ATP has OH on its surface, which
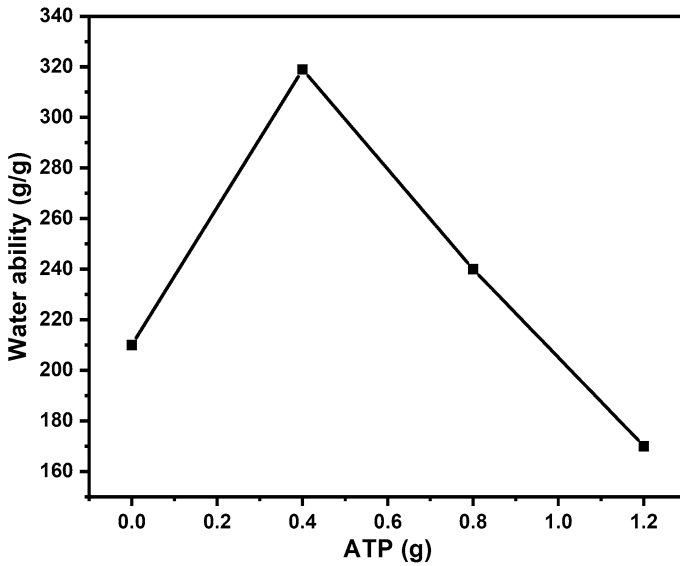
Fig. 7 Effect of ATP content

reacts with AM to strengthen the polymeric network, increasing the water absorption as a result. For instance, the swelling improved from 210 to 319 g/g when the ATP amount was raised by up to 0.4 g. Nevertheless, the swelling ability fell to 170 g/g as the clay amount was elevated additional, to 1.2 g. Further crosslink
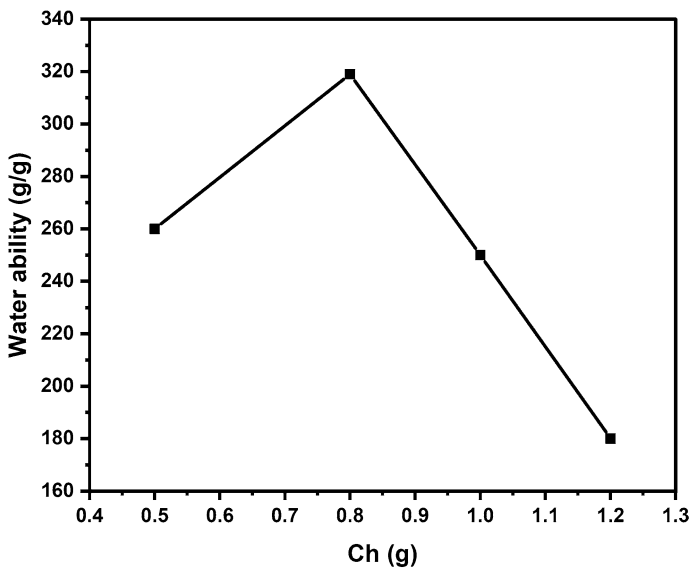

Fig. 8 Effect of Ch amounts

places were formed as ATP content increased, which produced the composite to contract.

The effect of chitosan content

Ch in various concentrations ranging from 0.5 to 1.5 g was added to the composite to examine the impact of the CTS quantities on the swelling (Fig. 8). The findings indicated that adding 1.5 g of Ch to the composite resulted in a decrease in swelling ability. This may be because the ratio of AM monomer to KPS has decreased, which has an impact on the grafting of small amounts of AM. Another way to put it is that while the amount of accessible AM monomer is constant, adding more chitosan dilutes the AM.

Effect of medium pH

At room temperature, the pH of the aqueous medium was diverse to determine the impact of pH on swelling ability (Fig. 9). Since the ionic strength affects how much an anionic superabsorbent swell, no further counter ions (cations) were presented to the buffer solution to set pH. The findings demonstrated that the swelling of ATP2 enlarged as pH rose to 3.0 because of the presence of several interaction species in the swelling medium that is pH-dependent, and subsequently reduced in the pH range of 3–6 due to the impact of the counter ions. The carboxylic acid component as well as Cl$^-$ work to shield the K cations' charge and prevent effective repulsion. The swelling increased dramatically as the pH level rose to 8. This might be a result of the carboxylate group becoming ionized, which increases swelling due to
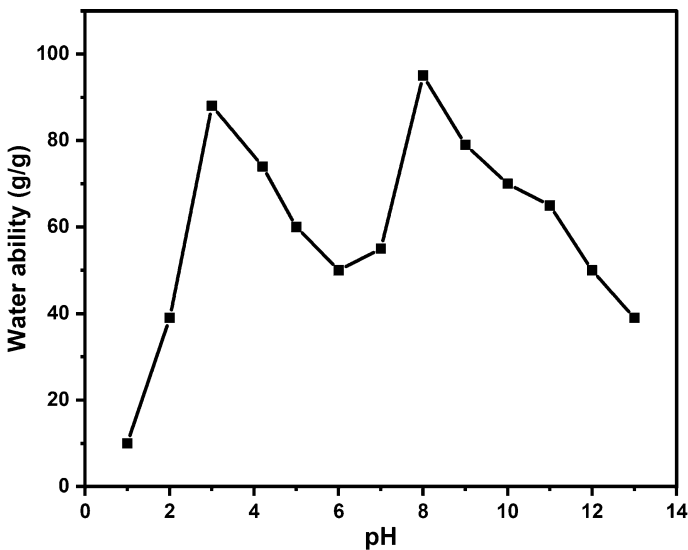

Fig. 9 Effect of pH

the electrostatic interaction among the charge sites (COO⁻). Again, at pH 9–13, a screening consequence of the counter ions Na^+ stops swelling [34].

Effect of saline solutions

The interaction of several saline solutions and the composite superabsorbent was studied since external saline solutions have a significant impact on the water absorption capacity of superabsorbent. The effect of NaCl, $CaCl_2$, and $FeCl_3$ on the water absorption is depicted in Fig. 10.

By increasing the three-salt solution concentration, the water absorbency falls. The screening impact of penetration counter ions Na, Ca, and Fe on the anionic hydrophilic groups, which limits the growth of the polymeric network, made it clear that water absorbency diminishes with an increase in the ionic strength of the external solution [35].

Release of urea

Urea was released during a 15-h period utilizing a Biosystem device. The results showed that the release rate was late, and the release duration extended from 5 to 21 h when the amount of ATP in the formulation was raised from 0 g to 1.2 g (Fig. 11). The system displayed a comparatively high percentage of urea emission in the early hours. This is as a result of approximately urea molecules absorbing on the composite surface. Given that the coating composite has not yet reached the swelling equilibrium, the generated surface holes may have made it simple for water to penetrate to the urea contained in the core, resulting in the initial
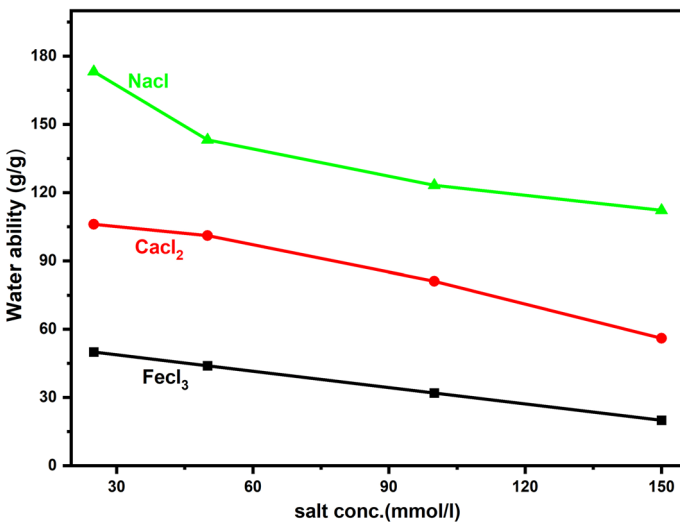

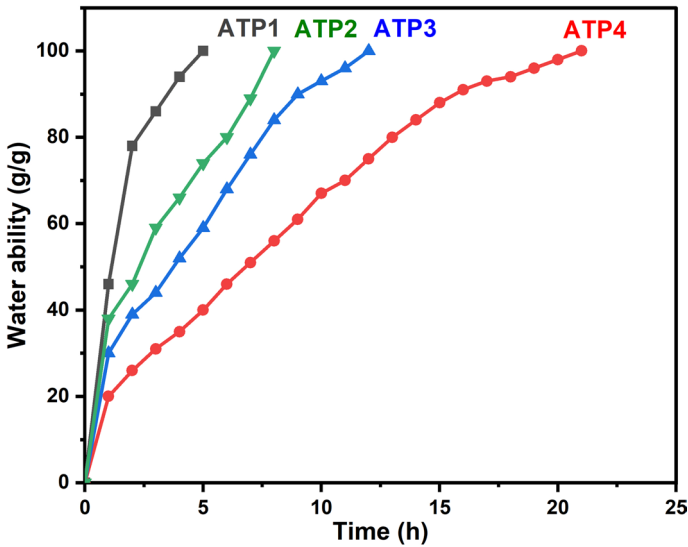**Fig. 10** Effect of saline solutions

Fig. 11 The urea release rate from composites has diverse ATP quantities

release of urea in the early hours. All of the surface pores may have closed after the swelling equilibrium has been established, causing the release of urea from control release urea fertilizer (CRUF) to proceed according to a diffusion process from the composite's interlayers.

By increasing the ATP content, a reduction in the released urea rate was observed because of the release is diffusion-controlled; as a result, as the percentage of ATP rises, more barriers are created, slowing down diffusion and, in turn, the pace at which urea is released. The ideal swollen was generated once the swelling balance was attained.

Conclusions

By employing KPS as an initiator and MBA as a crosslinker during the graft copolymerization of AM and chitosan in the presence of attapulgite clay, a unique series of superabsorbent composites were created. With a swelling of 319 g/g in distilled H_2O and 170 g/g in 0.9 wt.% NaCl solution, a superabsorbent composite was created. The rate of urea release was reduced as the amount of ATP in the composite increased, resulting in superabsorbent composites with urea slow-release functionality.

Availability of data and materials Not applicable.

Declarations

Competing interests The authors confirm that this publication does not encompass known disputes.

Ethics approval and consent to participate Not applicable.

Consent for publication Not applicable.

Open Access This article is licensed under a Creative Commons Attribution 4.0 International License, which permits use, sharing, adaptation, distribution and reproduction in any medium or format, as long as you give appropriate credit to the original author(s) and the source, provide a link to the Creative Commons licence, and indicate if changes were made. The images or other third party material in this article are included in the article's Creative Commons licence, unless indicated otherwise in a credit line to the material. If material is not included in the article's Creative Commons licence and your intended use is not permitted by statutory regulation or exceeds the permitted use, you will need to obtain permission directly from the copyright holder. To view a copy of this licence, visit http://creativecommons.org/licenses/by/4.0/.

References

1. Feng DJ, Bai B, Ding CX, Wang HL, Suo YR (2014) Synthesis and swelling behaviors of yeast-g-poly(acrylic acid) superabsorbent co-polymer. Ind Eng Chem Res 53:12760–12769
2. Puoci F, Iemma F, Spizzirri UG (2008) Polymer in agriculture: a review. Am J Agric Biol Sci 3:299
3. Kosemund K, Schlatter H, Ochsenhirt JL, Krause EL, Marsman DS, Erasala GN (2009) Safety evaluation of superabsorbent baby diapers. Regul Toxicol Pharm 53:81
4. Wang W, Li A, Zhang J, Wang A (2007) Study on superabsorbent composite. XI. Effect of thermal treatment and acid activation of attapulgite on water absorbency of poly(acrylic acid)/attapulgite superabsorbent composite. Polym Compos 28(3):397–404
5. Preisinger A (1961) Sepiolite and related compounds: its stability and application. Clays Clay Miner 10(1):365–371
6. Anitha A, Sowmya S, Kumar PTS, Deepthi S, Chennazhi KP, Ehrlich H, Tsurkan M, Jayakumar R (2014) Chitin and chitosan in selected biomedical applications. Prog Polym Sci 39:1644–1667
7. Wang Q, Zhang JP, Wang AQ (2009) Preparation and characterization of a novel pH-sensitive chitosan-g-poly (acrylic acid)/attapulgite/sodium alginate composite hydrogel bead for controlled release of diclofenac sodium. Carbohydr Polym 78:731
8. Goda E, Abu Elella M, Sohail M, Singu B, Pandit B, El Shafey AM, Aboraia A, Gamal H, Hong SE, Yoon R (2021) N-methylene phosphonic acid chitosan/graphene sheets decorated with silver nanoparticles as green antimicrobial agents. Int J Bio Macromol 182:680–688. https://doi.org/10.1016/j.ijbiomac.2021.04.024
9. Goda E, Abu Elella M, Sang E, Pandit B, Yoon R, Gamal H (2021) Smart flame retardant coating containing carboxymethyl chitosan nanoparticles decorated graphene for obtaining multifunctional textiles. Cellulose 28:5087–5105
10. Abu Elella M, Sabaa M, Hanna D, Abdel-Aziz M, Mohamed R (2020) Antimicrobial pH-sensitive protein carrier based on modified xanthan gum. J Drug Deliv Sci Technol 57:101673
11. Abu Elella M, Abdallah H, Gamal H, Moustafa E, Goda E (2022) Rational design of biocompatible IPNs hydrogels containing carboxymethyl starch and trimethyl chitosan chloride with high antibacterial activity. Cellulose 29:7317–7330
12. Kong M, Chen XG, Xing K, Park HJ (2010) Antimicrobial properties of chitosan and mode of action: a state of the art review. Int J Food Microbiol 144:51
13. Mellegard H, Strand SP, Christensen BE, Granum PE, Hardy SP (2011) Antibacterial activity of chemically defined chitosans: influence of molecular weight, degree of acetylation and test organism. Int J Food Microbiol 148:48

14. Dutkiewicz JK (2002) Superabsorbent materials from shellfish waste: aA review. J Biomed Mater Res A 63:373
15. De Jong WH, Borm PJ (2008) Drug delivery and nanoparticles:applications and hazards. Int J Nanomed 3:133–149. https://doi.org/10.2147/IJN.S596
16. Zhang J, Wang Q, Wang A (2007) Synthesis and characterization of chitosan-g-poly(acrylic acid)/attapulgite superabsorbent composites. Carbohy. Pol. 68:367–374. https://doi.org/10.1016/j.carbpol.2006.11.018
17. Ni XY, Wu YJ, Wu ZY, Wu L, Qiu GN, Yu LX (2013) A novel slow-release urea fertilizer: physical and chemical analysis of its structure and study of its release mechanism. Biosyst Eng 115:274–282
18. Azeem B, Kushaari K, Basit A, Man ZB, Thanh TH (2014) Review on materials and methods to produce controlled release coated urea fertilizer. J Control Release 10(181):11–21
19. Zohuriaan-Mehr MJ, Omidian H, Doroudiani S, Kabiri K (2010) Advances in non-hygienic applications of superabsorbent hydrogel materials. J Mater Sci 45:5711–5735
20. Golbashy M, Sabahi H, Allahdadi I, Nazokdast H, Hosseini M (2017) Synthesis of highly intercalated urea-clay nanocomposite via domestic montmorillonite as eco-friendly slow-release fertilizer. Arch Agron Soil Sci 63:84–95
21. Azlinawati Ramli R (2019) Slow release fertilizer hydrogels: a review. Polym Chem 10:6073–6090
22. Qin SH, Wu ZS, Rasool A, Li C (2012) Synthesis and characterization of slow-release nitrogenfertilizer with water absorbency: based on poly(acrylicacid-acrylic amide)/na-bentonitem. J Appl Polym Sci 126:1687–1697
23. Hsu SC, Don TM, Chiu WY (2002) Free radical degradation of chitosan with potassium persulfate. Polym Degrad Stab 75:73
24. El-araby A, El Ghadraoui L, Errachidi F (2022) Physicochemical properties and functional characteristics of ecologically extracted shrimp chitosans with different organic acids during demineralization step. Molecules 27:8285
25. Patel HA, Somani RS, Bajaj HC, Jasra RV (2007) Fabrication of reusable temperature-controlled-released fertilizer using a palygorskite-based magnetic nanocomposite. Appl Clay Sci 35:194
26. Zhang J, Wang L, Wang A (2007) Preparation and properties of chitosan-g-poly(acrylic acid)/montmorillonite superabsorbent nanocomposite via in situ intercalative polymerization. Ind Eng Chem Res 46:2497
27. Wang XY, Du YM, Yang JH, Wang XH, Shi XW, Hu Y (2006) Preparation, characterization and antimicrobial activity of chitosan/layered silicate nanocomposites. Polymer 47:6738
28. Liu J, Wang A (2008) Study on superabsorbent composites. XXI. Synthesis, characterization and swelling behaviors of chitosan-g-poly(acrylic acid)/organo-rectorite nanocomposite superabsorbents. J Appl Polym Sci 110:678
29. Douglas DB, Sergio PCF (2004) A kinetic study on the thermal degradation of N, N, N-trimethyl-chitosan. Polym Deg Stab 84:353–361
30. Aly K (2004) New polymer syntheses XXVIII. Synthesis andthermal behavior of new organometallicpolyketones and copolyketones basedon diferrocenylidenecyclohexanone. J Appl Polym Sci 94:1440–1448
31. Abd-alla MA, Aly KI (1991) Arylidene polymers. IX. Synthesis, characterization, and morphology of new polyesters of diarylidenecycloalkanones containing thianthrene units. J Macromol Sci Part A: Chem, 28: 251–267.
32. Kamal IA (2000) Liquid crystalline polymers. 3. Synthesis and liquid crystal properties of thermotropic poly(arylidene-ether)s and copolymers containing cycloalkanone moiety in the polymer backbone. J Macromol Sci Part A Pure Appl Chem 37:93–115. https://doi.org/10.1081/MA-100101083
33. Kenawy E, Azaam M, El-nshar E (2018) Preparation of carboxymethyl cellulose-g-poly (acrylamide)/montmorillonite superabsorbent composite as a slow-release urea fertilizer. Polym Adv Technol 29:2072–2079. https://doi.org/10.1002/pat.4315
34. Kenawy E, Seggiani M, Cinelli P, HasabElnaby H, Azaam M (2020) Swelling capacity of sugarcane bagasse-g-poly(acrylamide)/attapulgite superabsorbent composites and their application as slow release fertilizer. Euro Polym J 133:109769. https://doi.org/10.1016/j.eurpolymj.2020
35. Kenawy E, Seggiani M, Hosny A, Rashad M, Cinelli P, Saad-Allah K, El-Sharnouby M, Shendy S, Azaam M (2021) Superabsorbent composites based on rice husk for agricultural applications: Swelling behavior, biodegradability in soil and drought alleviation. J Saudi Chem Soc 25:101254. https://doi.org/10.1016/j.jscs.2021.101254